Oscillatory and transient flow modes in block nozzle arrangements with a base region

Pavel Bulat[1, *], Katerina Komar[1], Nickolay Prodan[1], Konstantin Volkov[2]
[1]Baltic State Technical University, St Petersburg, Russia
[2]Kingston University, London, United Kingdom

Abstract

Multi-jet interactions are characterised by a number of shock and expansion waves, formation of turbulent shear layers and subsonic recirculation zones. The problem of the occurrence of unsteady, transient and oscillatory, processes arising in the nozzle devices of rocket engines at different flight modes is discussed. The main flow regimes, the sequence of their change and qualitative patterns of shock-wave structures that arise in each of the regimes are considered. The main emphasis is paid to the causes of occurrence and mechanisms of maintenance of low-frequency oscillations of the base pressure. The regularities of changes in the amplitude-frequency characteristics of oscillations are studied depending on the main parameters of the problem. Areas of existence of oscillatory processes are found, and a search is carried out for the ranges of design parameters, geometric characteristics of nozzle assemblies that provide a non oscillating flow of gas-dynamic processes. Hysteresis phenomena of shock-wave structure at increase or decrease in the reservoir total pressure is observed.

Keywords

Flight safety; nozzle; base pressure; pressure oscillations; multi block jet; shock wave

1. Introduction

To overcome challenges facing aerospace industry and to provide space flight safety of commercial space launch vehicles and their components it is required to accelerate the design process and reduce preliminary development testing. The space launch vehicle passes through several phases of flight before reaching the desired target conditions in space. These phases of flight have unique modeling requirements that must be addressed by taking into account various physical phenomena (turbulence, recirculation regimes, gas dynamic discontinuities etc). Accurate definition of flow-induced pressure loads can be achieved before actual hardware testing through the use of experimental facilities and computer-based techniques.

The world has intensified work on commercial ultra-light launch vehicles. The service market in this area imposes severe cost constraints. As a result, the requirements for the aerodynamics of missiles and the specific thrust of the liquid-propellant engine in the atmospheric flight are becoming more stringent [1]. The desire to reduce the costs of developing liquid-propellant rocket engines leads to multi-engine layouts (Figure 1) with typical single-nozzle rocket engines in the first stage, and with the installation of one of the same engine in the second stage, but with a high-altitude nozzle. Unsteady interaction of supersonic jets exhausted from multi-nozzle unit significantly affect rocket base and launch facility. Rocket engines are subject to pressure oscillations caused by vortex shedding and acoustic feedback resulting from impingement of the vortices on the nozzle and other obstacles [2, 3].

a)

b)

Figure 1. Multi-nozzle assemblies proposed by Electron Rocket Lab (a) and assemblies with a truncated central body (b)

The use of multi-nozzle liquid-propellant rocket engines with a central body, usually truncated, and extendible nozzles with a rupture of the generatrix seems to be promising. Hypothetical designs of such engines are shown in Figure 2.

a)

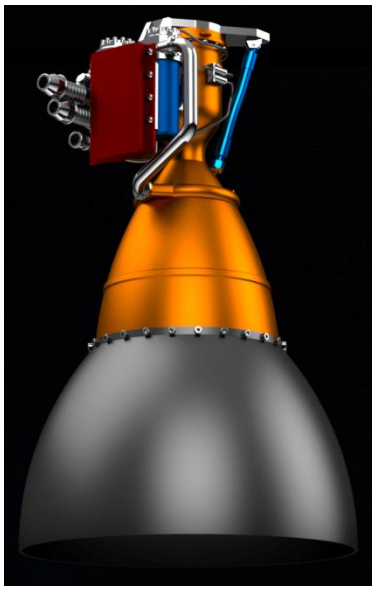

b)

Figure 2. Nozzle with a rupture (a) and a kink (b) of the generatrix

The base pressure oscillations and complex unsteady processes in the base region are typical for multi-block solutions. These processes are unsteady (transient and oscillatory), posing a danger to the rocket, especially at the moment of launch. Thus, the formulation of the problem of finding nozzle configurations, in which the restructuring of the jets occur in non-oscillating manner, is relevant.

It is obvious that all types of interactions of jets with each other and with structural elements in the arrangements shown in Figures 1 and 2 can be reduced to the following types of interactions: interaction of a single jet with the channel walls, interaction of an annular jet with the base of the central body, interaction of the jets with each other. Finally, for a block of nozzles, when one nozzle is located in the centre (Figure 1a), and the others are located rather tightly in a circle, it is assumed that the jet of the inner nozzle flows into a channel with solid walls.

Theoretical methods of calculation on base pressure in transonic and supersonic flow are developed in [4, 5]. A family of studies on flows in plane and axisymmetric channels for circular

and annular jets was carried out in [6–9]. The results of visual investigations of currents using interferograms in plane transparent channels and measurements using inertia-free sensors made it possible to reveal the existence of oscillatory modes of change in the bottom pressure and rearrangement of the wave structure. Low-frequency oscillations of the base pressure are discovered in [10, 11].

Classification of flow regimes, stationary, oscillating and transient, is given in [12]. Visualization of the flow and refinement of experimental data using numerical calculations made it possible to determine five typical shock-wave structures that arise when a jet outflows into a channel with a sudden expansion, as well as the sequence of their change with increasing and decreasing total pressure [12]. A control method is developed in [13] to suppress pressure oscillations induced by supersonic cavity flow using high-speed upstream injection.

An experimental investigation of an airflow from convergent-divergent axisymmetric nozzles expanded suddenly into circular duct is carried out in [14]. Numerical analysis is performed in [15] to provide the efficacy of the supersonic Mach numbers due to the flow from supersonic nozzle exhausted in a larger circular duct. The experimental analysis in [16] is performed for various nozzle pressure ratios, length to diameter ratios and area ratios.

The interaction of supersonic underexpanded jets for a four-nozzle clustered rocket configuration is studied in [17] using three-dimensional Reynolds-averaged Navier–Stokes (RANS) equations. The k-omega turbulence model is used to capture the physics of shock-turbulence interaction and its effect on the multi-jet flowfield. Three-dimensional simulation based on RANS equations is carried out in [18] to explore the unsteady flow in over-expansion regime. Prediction of the side load level in an overexpanded nozzle within a forced oscillation regime is carried out in [19]. The calculations exposed in the study point out a critical frequency of oscillation of the nozzle at which the shock motion and the side load level observed have maximum values.

A numerical investigation is conducted in [20] in order to identify the flow separation behaviour. The evolution of the shock structure and flow separation region with an increase in the nozzle pressure ratio is reported. The prediction of the separation data on the nozzle wall and the influence of the gas density on the flow separation are also part of the study. The spectral analysis performed in [21] captures typical wake flow frequencies and their characteristic mode shape for the cross-flapping and swinging motion of the ambient shear layer. A strong amplification of the swinging motion is observed at certain conditions. It is governed by a coupling of the dynamic wake flow modes and the acoustic chamber properties. The phenomenon of a turbulent boundary layer separation from the rocket engine nozzle wall intensively studied in the overexpansion mode in [22].

The application of dual-bell nozzles to existing space launchers offers the possibility to significantly increase their payload capability. This benefit is related to the ability of this kind of nozzles to switch between a low-altitude and a high-altitude working mode. However, the transition between the working modes introduces several problems like for example the possible development of high side-loads and a significant jump in the thrust magnitude. Using a preliminary calibration of a modified version of the Spalart–Allmaras turbulence model, the effects of the injection on the transitional nozzle pressure ratio are investigated in [23]. In [24], RANS equations at steady state conditions are solved with an in-house CFD tool. The study allows to investigate the flowfield and determine the required secondary mass flow rate for which the control is effective.

Different turbulence modelling strategies are applied in [25] including steady-state RANS and unsteady RANS (URANS) simulations based on two-equation models as well as a hybrid URANS/LES approach (Delayed Detached-Eddy Simulation). The frequencies and amplitudes of the first four longitudinal modes measured in the experiment were satisfactorily reproduced with URANS simulations with the k-omega model. The flame oscillation characteristics are investigated experimentally in [26]. The interactions between self-pulsation, flame oscillation as well as pressure oscillations of manifold and combustor are analyzed. The results of computer

code developing, verification and validation, making it possible to simulate unsteady processes of ignition and combustion in rocket engines are reported in [27].

A model of a self-oscillating process arising from the interaction of a non-isobaric jet with semi-closed cylindrical cavities is considered in [28, 29]. This model allows to identify typical elements of the gas-dynamic structure of the forming flow. The physical pattern of the flow in the gas–jet generator has been discussed and the study of the dependence of the self-sustained oscillation characteristics on the key gas-dynamic and geometric parameters has been performed.

This study focuses on experimental and numerical investigations of supersonic separated flows in channel with sudden expansion. These flows are typical for many rocket engines with multi-nozzle arrangements. The main flow regimes, the sequence of their change and qualitative patterns of shock-wave structures that arise in each of the regimes are considered. The main emphasis is paid to the causes of occurrence and mechanisms of maintenance of low-frequency oscillations of the base pressure. The regularities of changes in the amplitude-frequency characteristics of oscillations are studied depending on the main parameters of the problem.

2. Experimental method

Experimental study of a single and annular jet flowing into a cylindrical channel with a sudden expansion is carried out. The flow in the channel is characterized by the parameters shown in Figure 3. The base pressure is measured by inertia-free sensors directly on the base. The geometry of the installation is determined by the Mach number at the nozzle exit (M_a), nozzle exit diameter (d_a), pipe diameter (d_{tb}), nozzle throat diameter (d_*), nozzle length (l_{nz}), long pipe (l_{tb}), nozzle half-opening angle (θ_a). In the experiments, we used a channel with a diameter of 85 mm and a nozzle with a nozzle throat diameter of 10.6 mm. The total excess pressure in front of the nozzle rose from 0 to about 120 bar at a rate of about 5 bar per second. Then the pressure was quickly released, i.e. hysteresis of the change of modes during the rise and fall of the total pressure has not been studied.

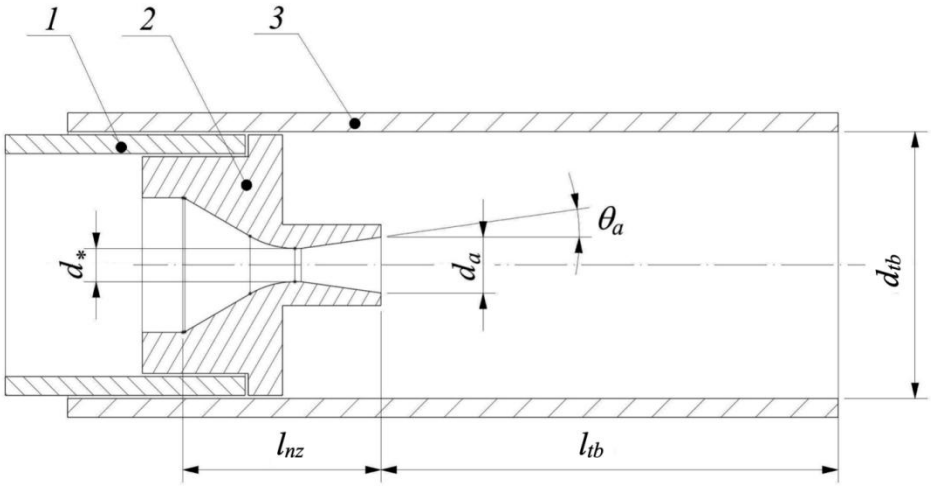

Figure 3. Scheme of an axisymmetric jet exhausted into a channel with a base region, where 1 is receiver, 2 is supersonic nozzle, 3 is cylindrical pipe (d_a is nozzle outlet diameter, d_{tb} is pipe diameter, d_* is nozzle throat diameter, l_{nz} is nozzle length, l_{tb} is pipe length, θ_a is nozzle half-opening angle)

The nozzle blocks has replaceable cylindrical nozzles of various lengths. The nozzles with outlet Mach numbers M_a=2 and 3 and nozzle angles θ_a=8, 15 and 40° are used. The critical section of the Laval nozzle is d_*=30 mm, the width of the annular throat of the nozzle is 5.3 mm, the pipe diameter is d_{tb}=85 mm. The experiments are carried out in cold air at a temperature of T=300 °C.

3. Numerical method

Various turbulence models are verified before carrying out the computational experiment. Test calculations are carried out for a supersonic jet flowing from a circular nozzle into a flooded space at a ratio of pressure at the nozzle outlet p_a to the ambient pressure p_h ($n=p_a/p_h$) typical for a non-self-similar regime. The calculations were performed by the settling method until the mesh convergence is achieved for each turbulence model separately.

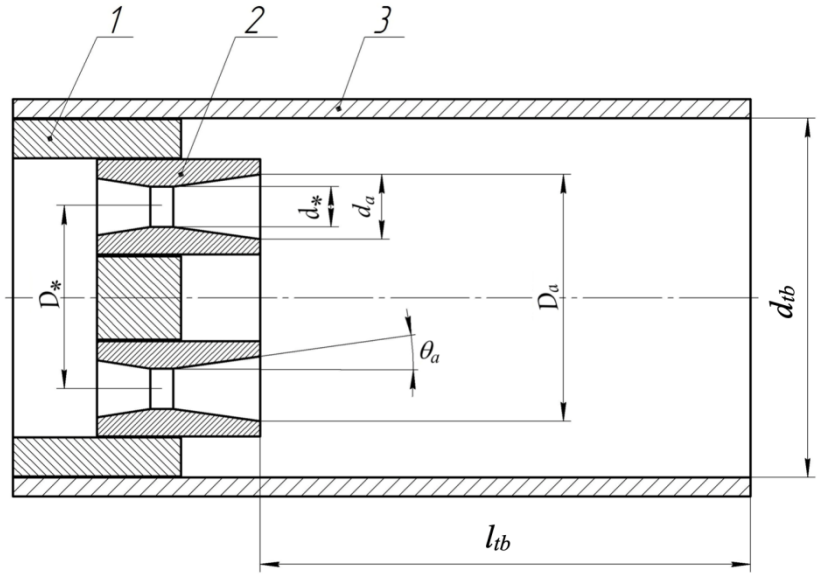

Figure 4. Scheme of a jet exhausted from an annular nozzle into a channel with a base area, where 1 is nozzle block, 2 is annular nozzle, 3 is channel with sudden expansion (d_* is width of the annular throat of the nozzle, D_* is diameter of the median line of the annular nozzle, d_a is width of the outlet section of the annular nozzle, D_a is outer diameter of the nozzle, d_{tb} is pipe diameter, l_{tb} is pipe length)

The numerical problem is solved in an axisymmetric formulation [30]. The two-dimensional computational domain is divided by a structured computational mesh consisting of quadrangular cells. The computational mesh consists of 180 thousand elements (200 elements are used in the nozzle throat). Discretization of governing equations is carried out using finite volume method and upwind scheme of the second order of accuracy, which make it possible to increase the order of approximation of the flow quantities without losing the monotonicity of the solution. An implicit time sampling scheme is used. The Roe method is used as a scheme for splitting the flux differences.

The total pressure and the static pressure, which provides the flow velocity with the Mach number equal to unity in the nozzle throat, are applied to the outlet boundary. The pressure is set equal to atmospheric on the outlet boundary.

Figure 5 and Table 1 show the results of the calculations. The Transition SST model better predicts the position of the Mach disk in the jet, since the flow in front of it is hypersonic and almost laminar. In the peripheral region, the SST model predicts the jet dimensions much better, and this factor is of decisive importance. The model of a perfect ideal gas is applied. The four-parameter RANS turbulence model SST, which is a hybrid model using k–epsilon and k–omega turbulence models, is used in further calculations. The realizable k–epsilon model is poorly predict the jet flowfield. The calculations with standard k-ε model run more stable, as the turbulent viscosity is calculated in a less complex way compared to its realizable version. The governing equations for the turbulent kinetic energy and its dissipation rate are highly non-linear in the realizable model and require a more careful numerical discretization.

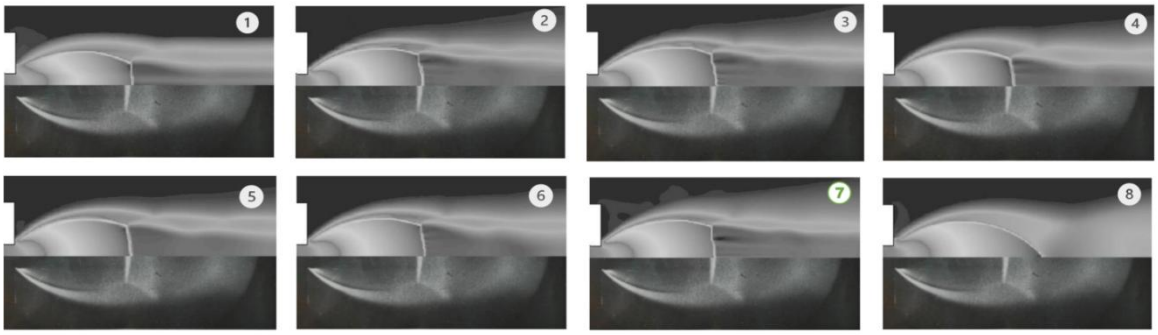

Figure 5. Results of testing various turbulence models for a supersonic submerged jet for M_a=1 and n=24, where 1 is model of inviscid gas, 2 is Spalart–Allmaras vorticity based model, 3 is Spalart–Allmaras strain/vorticity based model, 4 is k–epsilon model, 5 is k–omega model, 6 is k–omega SST model, 7 is transition SST model, 8 is k–epsilon Realizable model

Table 1. Comparison of the results computed with various turbulence models

Model	Location of Mach disc from the nozzle outlet	Relative error, %
Experiment	4.44	0
Model of inviscid flow	4.73	6
Spalart–Allmaras vorticity based model	4.59	3
Spalart–Allmaras strain/vorticity based model	4.60	4
k–epsilon model	4.75	7
k–omega model	4.61	4
k–omega SST model	4.74	7
Transition SST model	4.55	2
k–epsilon Realizable model	5.91	33

4. Results and discussion

Experimental and numerical results are reported for two cases, one of them corresponds to interaction of axisymmetric jet with tube cavity and another one corresponds to interaction of annular jet with tube cavity. The results are reported for various geometrical parameters of the problem and inlet flow quantities.

4.1. Flow pattern

Figures from 6 to 8 show schlieren photographs of experiments on various nozzle blocks. The most common case is a block jet with a number of nozzles larger than or equal to six, flowing into the channel (Figure 6). In this case, there are two base regions in the flow, formed by jets and outer walls. These flows are typical for the moment of engine operation, when the rocket is still on the launch pad, and the combustion products are discharged into the gas outlet channel.

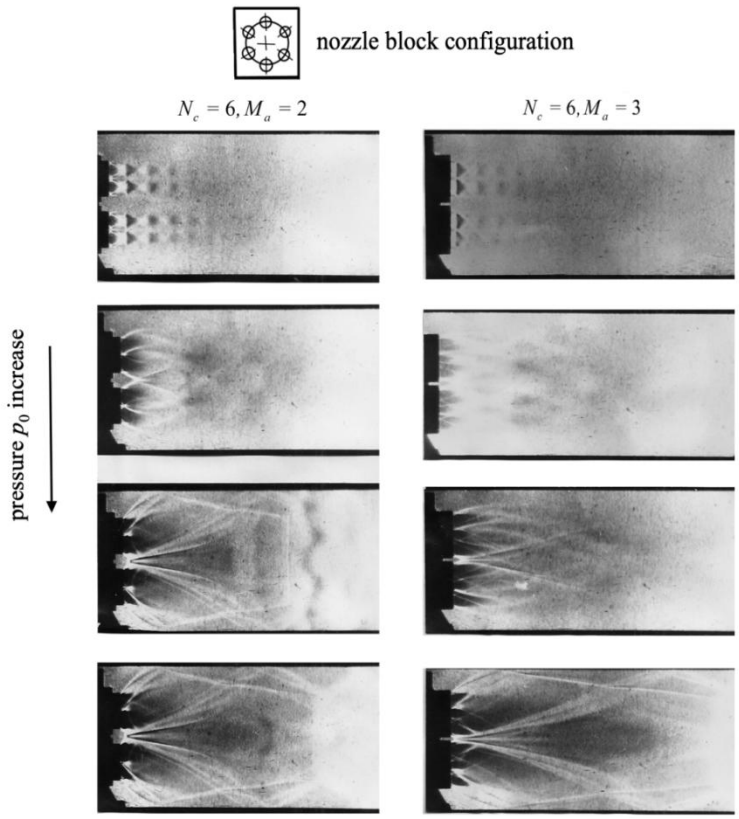

Figure 6. Visualization of the outflow of a block jet into a channel with a square cross section (N_c is number of nozzles, M_a is outlet Mach number)

When there are more than six nozzles, they form an annular jet. The structure of shock-wave structure of the multi-block jet presented in Figure 7 (10 nozzles are used) is similar to the structure of a plane jet flowing out of a block of nozzles (Figure 7).

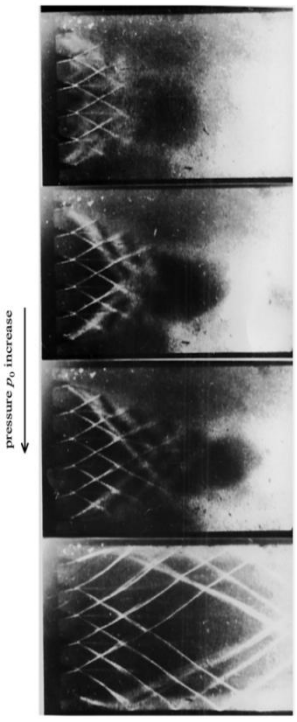

Figure 7. Visualization of the flow of a block jet with the arrangement of nozzles in a row for M_a=2

There are three main types of flow which are accompanied by gas exchange with the base area (Figure 8). These types include flow mode when the jet does not run onto the walls (the case of an open base region); flow mode when the jet flows onto the wall in a turbulent section (non-self-similar mode with a closed base region); flow mode when the jet flows onto the wall in a supersonic section (self-similar regime with a closed base region).

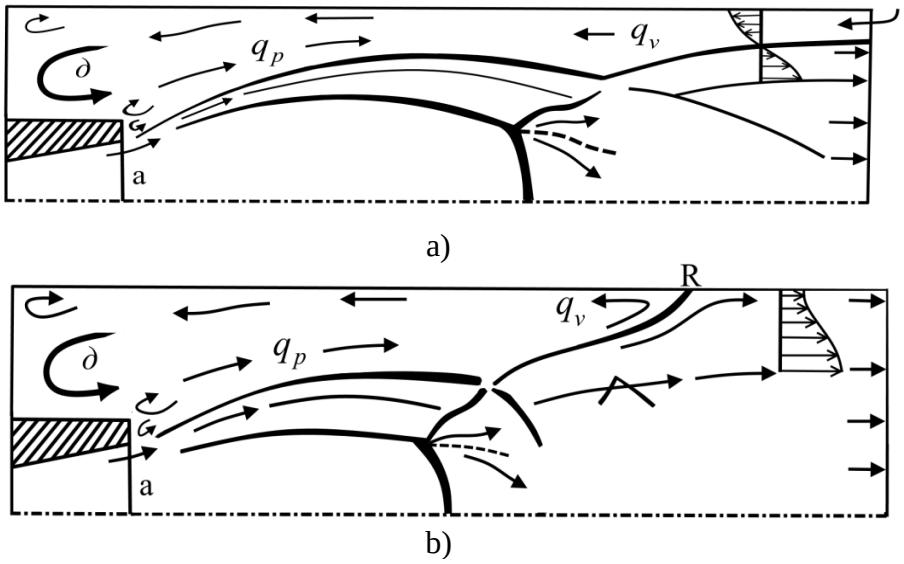

Figure 8. Open (a) and closed (b) base regions

If the base region is open (Figure 8a), then the ambient gas flows into it along the gap between the channel walls and the jet boundary with a flow rate q_v. At the same time, the jet ejects gas from the base area with a flow rate q_p. The quantity $\xi=(q_p-q_v)/Q_a$, where Q_a is the gas flow through the nozzle, is called the flow rate imbalance. The flow regime is steady state if $\xi=0$. In the case shown in Figure 8b, the ambient gas does not enter the base area. The pressure on the wall changes from the base p_b to the ambient pressure p_h. The velocity in the turbulent section of the jet decreases with distance from the axis. Accordingly, a part of the gas located above the slip line (point R in Figure 8b), the velocity head of which is insufficient to overcome the positive pressure gradient, turns into the base region.

The situation is more complicated when the jet flows onto the wall within its supersonic section. Figure 9 shows the results of numerical simulation of this case.

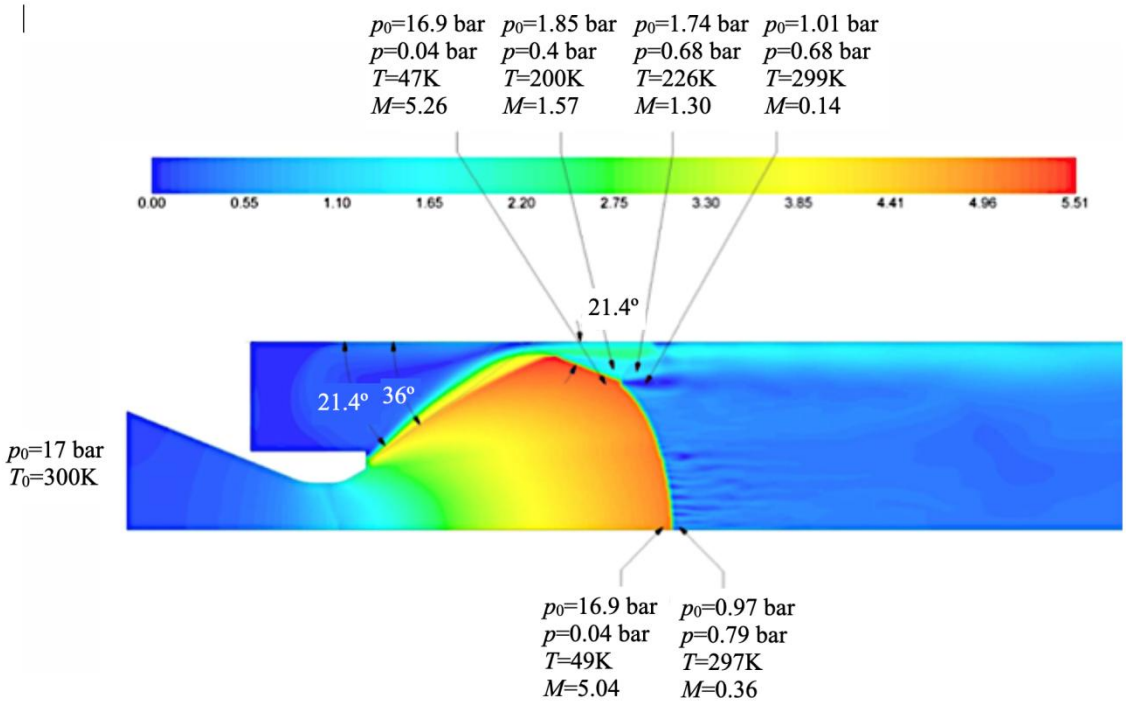

Figure 9. The flow pattern for the jet impinging onto the wall within the supersonic section for M_a=2 and θ_a=30°

The results of numerical simulation allow to reconstruct the physical pattern of the flow in the near-wall layer (Figure 10). In this figure, A is the point of inflow of the boundary of the ideal jet onto the wall, A_1 is the point of intersection of the boundary of the mixing layer with the wall, B is the point at which the curvature of the jet boundary begins under the influence of pressure waves propagating from the wall, N is the boundary of an ideal gas, N' is a wall shock.

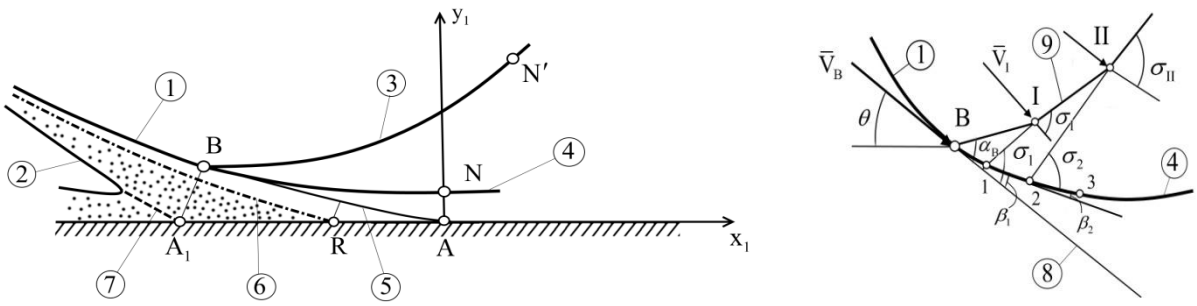

a) b)

Figure 10. Flow pattern (a) and mechanism of formation (b) of wall hanging shock (α is the angle of inclination of the characteristic to the streamline, β is the angle of flow turn, σ is the angle of inclination of the jump to the streamline, θ is the angle of inclination of the velocity vector). Here, 1 is the boundary of the jet of ideal gas, 2 is the boundary of the mixing layer, 3 is the wall shock, 4 is the line of maximum flow rates, 5 is the continuation of the conventional boundary of the ideal gas jet as it would be in the absence of the wall, 6 is the gas deploying to the base area, 7 is the continuation of the conventional boundary of the mixing layer, 8 is the continuation of the streamline, 9 is the hanging shock formation

Between the boundary of the ideal gas 1 and the boundary of the mixing layer 2, a viscous flow takes place. The pressure remains approximately constant in the cross sections of this layer, and the velocity decreases from a maximum value at boundary 1 to zero at boundary 2. There is a conditional flow separation line inside the mixing layer, which intersects with a wall at the stagnation point R. The entire flow below this line turns to the base area, the flow above

overcomes the positive pressure gradient and flows between the wall and the boundary of the ideal gas jet N. Point A_1 (the intersection with the wall of the conditional line 7) is a continuation of the boundary of the mixing layer, from which the characteristic (disturbance wave) A_1–B propagates, intersecting with the boundary of the ideal gas at point B. This is a discontinuous characteristic, i.e. it is a gas-dynamic discontinuity of the first order (up to point A_1, the pressure gradient on the wall is equal to zero, and on the A_1–B characteristic itself it abruptly acquires a positive value). At the point B, under the influence of the discontinuity of the pressure gradient, the curvature of the streamline breaks down, which leads to the nucleation at some distance from the point B of the hanging shock 3 (at the point I), which is usually called the wall shock. Under the influence of a positive pressure gradient, the boundary of the ideal gas 4 is curved (the angle of flow rotation $\beta_2<\beta_1$ leads to the fact that the angle of inclination of the weak discontinuity increases $\sigma_2>\sigma_1$, which leads to the curvature of the wall shock).

If the jet flows into the wall in a supersonic section, then the entire flow field is supersonic below the inlet cross section. The pressure in the base area does not depend on environmental conditions; therefore, this mode is called self-similar. All other modes are non self-similar.

4.2. Base pressure

Figure 11 shows plots of base pressure against total pressure, which gives an idea of the most typical cases of the outflow of a supersonic jet into a channel of various lengths. The Mach numbers M_a=3 and 4 are chosen as characteristic for the nozzle blocks of the first stages of the rocket.

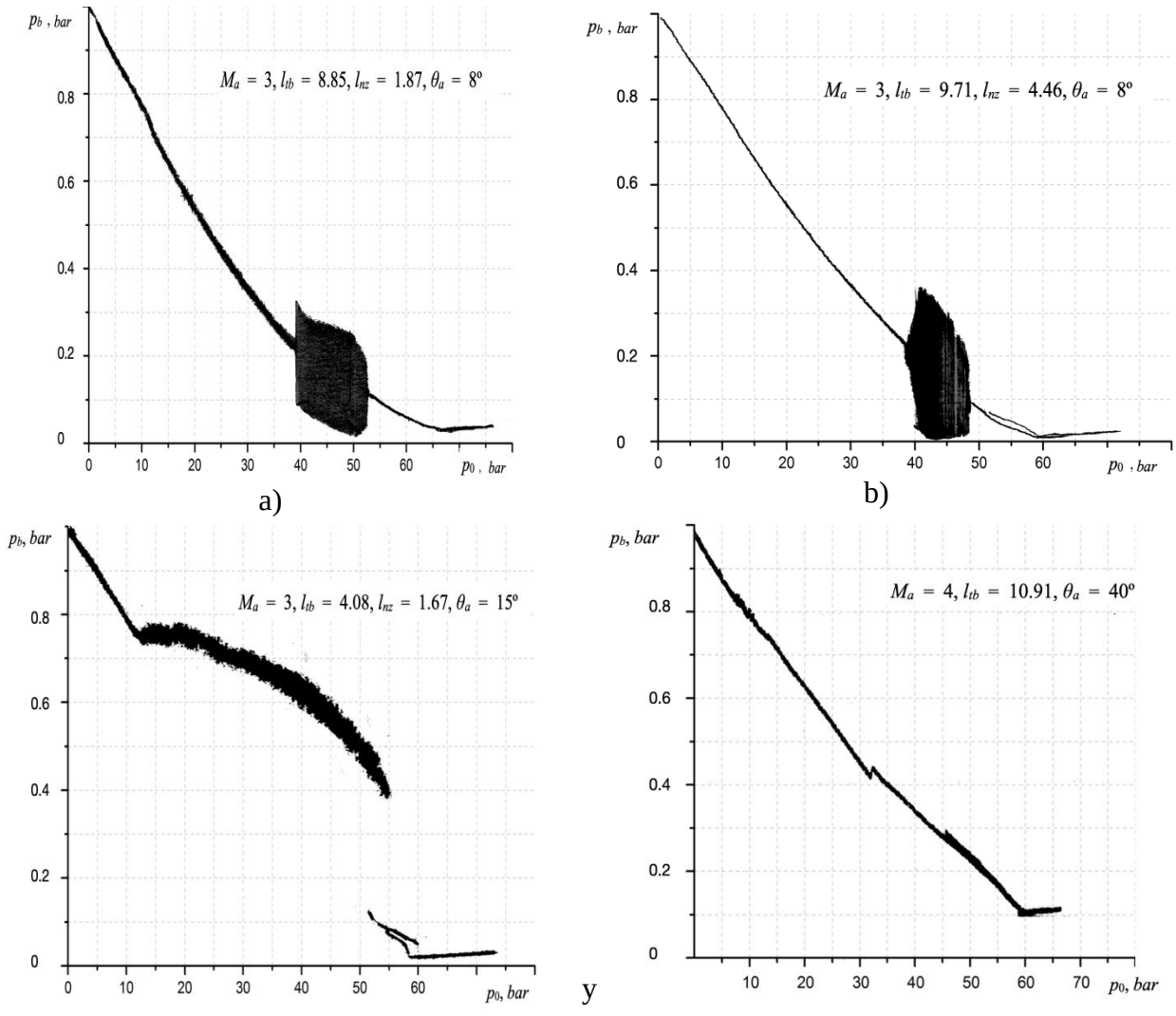

c) d)

Figure 11. Experimental dependencies of the base pressure on the pressure in front of the nozzle for the outflow of a jet into a pipe of various lengths

At a moderate angle of half-opening of the nozzle and a long tube, non-self-similar modes with an open and closed base region are separated by a region of oscillatory modes (Figures 11a and b). At approximately the same channel length, the development and termination of oscillations is strongly influenced by the nozzle carryover l_{nz}, i.e. the volume of the base area. When the base area is small (Figure 11a), the amplitude of oscillations at the beginning of the oscillatory regime increases sharply and also decreases rapidly when it ends. With a large volume of the base area, these processes are of a smoother gradual nature (Figure 11b). Figure 12c shows a plot for a relatively short channel. The end of the flow regime with an open base region occurs abruptly. The pressure in the base area drops almost instantly by about a factor of 2. Low frequency vibrations do not occur. Figure 11d shows the case of a jet outflow from a nozzle with a large half-opening angle into a long channel. All three main stationary regimes are present: 1) flow regime with an open base region, 2) flow regime a closed base region, 3) flow regime self-similar with a closed base region. Oscillations do not occur.

The graphs presented in Figure 11 show a hysteresis loop. With increasing and decreasing total pressure in the self-similar mode, the base pressure is the same, there is no hysteresis. However, switching from self-similar to non-self-similar mode when the total pressure is released occurs at larger values of total pressure than with an increase in total pressure. Correspondingly, when total pressure is reset, the graph line in non-automotive mode goes higher.

4.3. Unsteady and transient flow regimes

Analysis of the experimental plots of base pressure changes over time, as well as the results of numerical simulation, make it possible to classify unsteady flow modes (Figures 12 and 13). Figure 12 shows possible types of unsteady processes detected experimentally or by calculation. Depending on the geometry of the pipe and nozzle, some of the modes may be absent or poorly expressed. In the channels of medium length, there are no modes of low-frequency flow oscillations (line 2 in Figure 13). In short channels, there is also no non-self-similar mode with a closed base area (line 1 in Figure 13). Thus, the presence of certain flow modes can serve as a classification feature depending on the channel length. If all modes are present, then the channel is considered long. If there is no non-self-similar mode with a closed base area, then the channel is considered short. The rest of the channels are considered average.

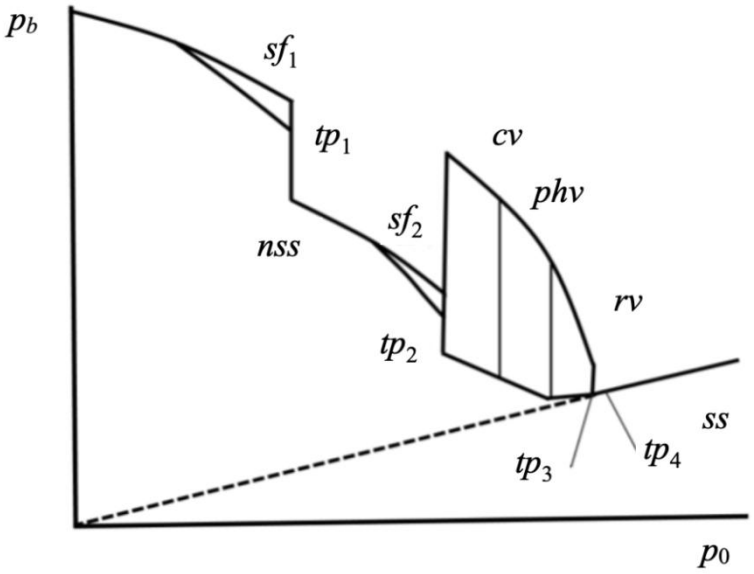

Figure 12. Classification of flow regimes on the $p_b(p_0)$ plot in the case of long channels, where *ss* is self-similar mode with a closed base area; *nss* is non-self-similar mode with a closed base area; sf_1 is stochastic oscillations with an open base area (obv), preceding the transition to *nss*; sf_2 is stochastic oscillations with a closed base area (cbv), preceding the transition to the mode of flow rate oscillations; *cv* is combined oscillations; *pgv* is pseudo-harmonic oscillations; *rv* is relaxation oscillations; tp_1 is transition process between obv and cbv modes; tp_2 is transient process corresponding to the beginning of the flow rate oscillations; tp_3 is transient process corresponding to the end of flow rate oscillations; tp_4 is transition mode between non-self-similar and self-similar modes

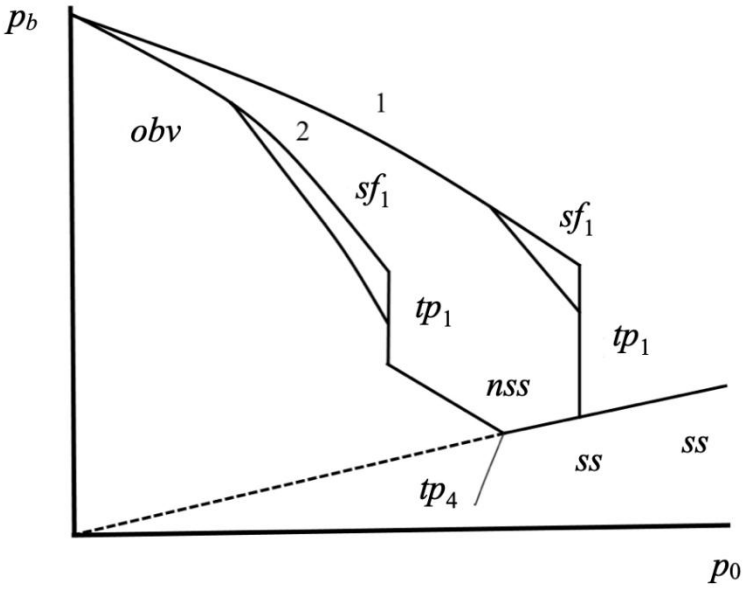

Figure 13. Typical plots of base pressure against total pressure for short (line 1) and medium (line 2) channels

It should be noted that in the self-similar mode, the base pressure depends linearly on the total pressure, and a straight line passes through the origin, which corresponds to a constant jet off-design. All other modes are non-self-similar, i.e. channel flow depends on environmental conditions.

4.4. Low-frequency oscillations

Figure 12 shows three types of low-frequency flow rate oscillations, which differ both in the form of the oscillatory cycle and in the physical mechanism of their maintenance. All of them are called flow rate oscillations, because are caused by an imbalance in the flow rates of gases flowing into and out of the base area. Figure 14 shows a plot obtained by calculation, in which all the described modes are present.

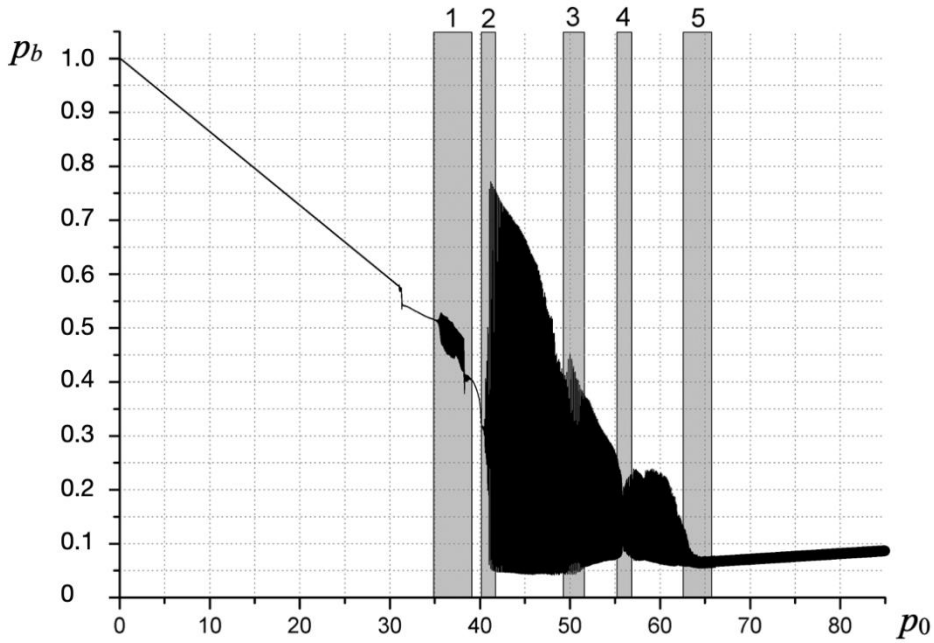

Figure 14. Dependence of base pressure on total pressure for M_a=3, θ_a=8°, l_{tb}=16.8, where 1 is stochastic oscillations sf_1, 2 is transient process tp_2, 3 is transition from composite oscillations *cv* to pseudo-harmonic *phv*, 4 is transition from *phv* to relaxation oscillations *rv*, 5 is transient process from *rv* to self-similar mode *ss*

The first type of vibration is called combined oscillations (*cv*), because part of the oscillatory cycle falls on the flow with an open base area, and part of oscillations falls on the flow with a closed base area (Figure 15). The oscillatory cycle visually consists of two fragments. Pseudo-harmonic oscillations (*phv*) occur with a completely closed base region (Figure 16). The jet interacts with the walls in a turbulent section.

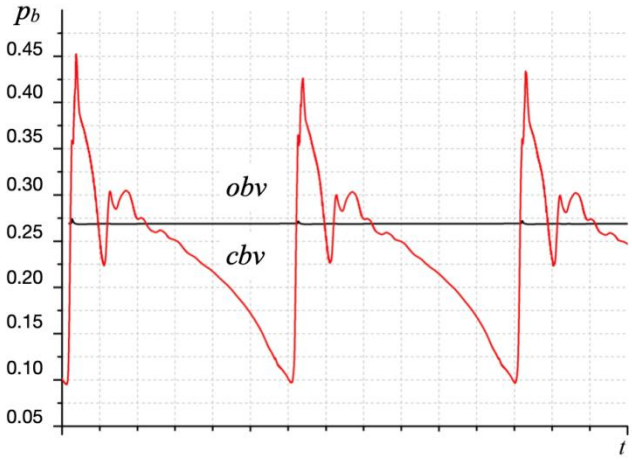

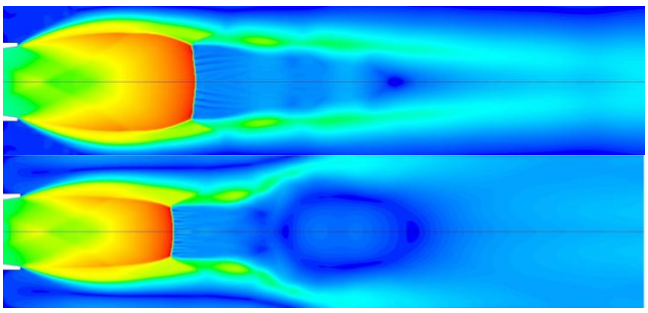

Figure 15. The type of oscillatory cycle typical for combined oscillations (*cv*), M_a=3, θ_a=8°, l_{tb}=16.8, p_0=45 bar

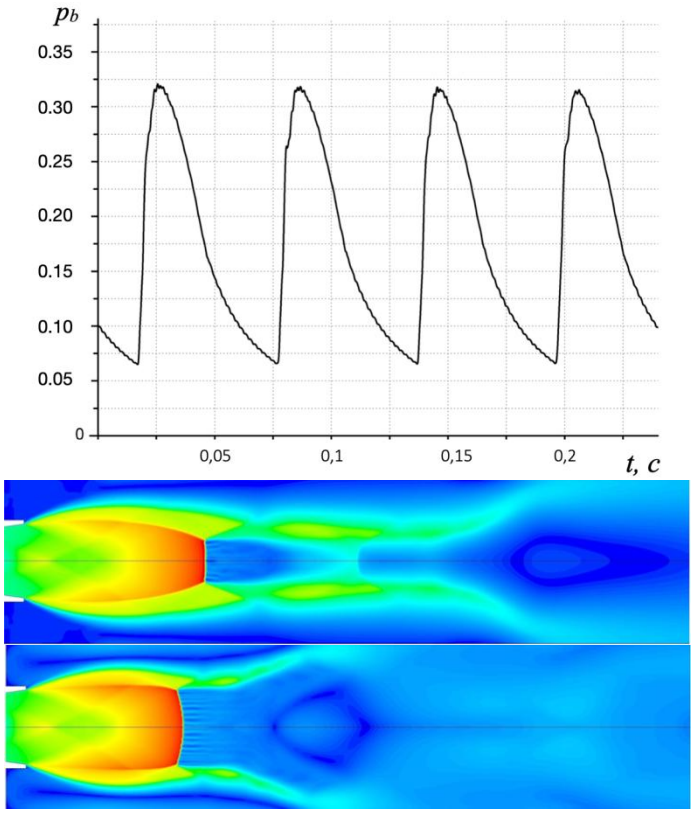

Figure 16. Pseudo-harmonic oscillations (*phv*), M_a=3, θ_a=8°, l_{tb}=16.8, p_0=52 bar

With a further increase in the total pressure in front of the nozzle, the oscillations pass to the relaxation type (*rv*). The shape of the cycle becomes sawtooth (Figure 17). At the minimum base pressure, the jet flows onto the wall within the first barrel with the formation of a curvilinear shock that overlaps the entire section of the channel. At this moment, the flow rate imbalance becomes positive and an intensive filling of the base area occurs, accompanied by an abrupt increase in the base pressure.

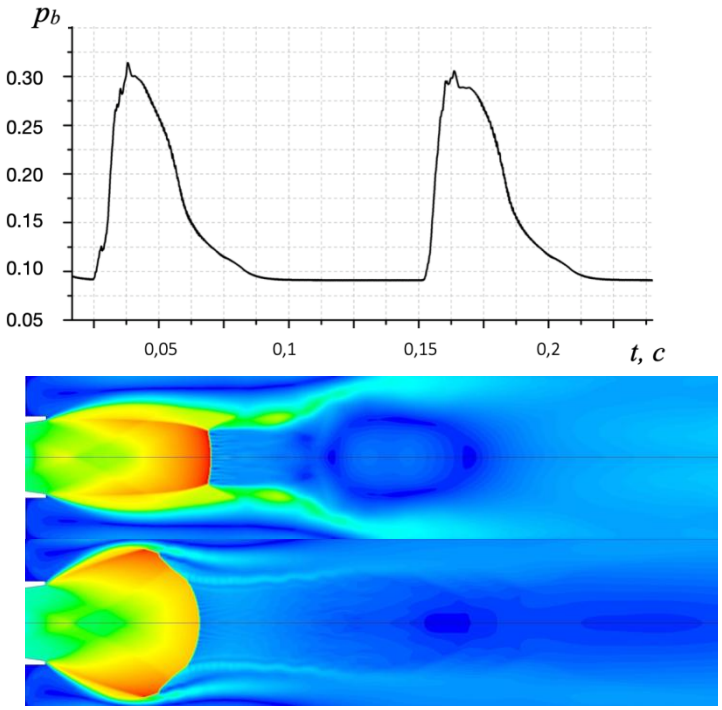

Figure 17. Relaxation oscillations (*rv*), M_a=3, θ_a=8°, l_{tb}=16.8, p_0=57 bar

Studies have shown that low-frequency oscillations acquire the most intense character in the case of a jet outflow from nozzles with M_a=3–3.5 and half-opening angle θ_a=8–15° into channels of medium length (l_{tb}=10–20).

When two parallel jets flow into a channel with a sudden expansion, the geometry and characteristics of the bottom region are different from the axisymmetric case with one jet. As a result of the intersection of two axisymmetric supersonic flows, a spatial shock-wave structure is formed, containing practically known types of interference of gas-dynamic discontinuities [31–35]. The parameters for the volume of the base area cannot be considered even approximately the same, since the base region itself is essentially three-dimensional. The nature of the flow and interaction of the mixing layers and supersonic flows with the walls in the plane of the nozzle axes and in the plane orthogonal to it are different. The base area can be divided into two communicating volumes, the zones between the nozzles and the rest of the base volume. The visualization of the flow shows that the region between the nozzles in both stationary and unsteady flow regimes remains approximately constant, while the peripheral flow region changes its size.

4.5. Smooth restructuring of the jet in the channel

The experimental results presented in Figures 11c and 11d show the restructuring of the shock-wave structure of a supersonic jet in the channel when the pressure in front of the nozzle changes is not always accompanied by the appearance of oscillations. In short channels, which in the case are a model of an aerospike nozzle with a truncated central body or a nozzle block with a central nozzle and peripheral nozzles closely spaced around a circle, the restructuring is accompanied by an abrupt change in the base pressure, which poses a danger to the rocket design. Figure 11d shows a graph corresponding to the outflow into a medium-length channel, when the restructuring occurs smoothly, without fluctuations and surges in the base pressure. This behaviour of the jet is favourable. To study the possible ranges of the parameters of the nozzle block, within which the restructuring of the jets can occur without oscillations, additional experiments were carried out and calculations were performed for nozzles with M_a=2–3. The results revealed the following pattern. If the nozzle has a half-opening angle θ_a>40°, then

oscillations in channels of medium and long length do not arise (Figure 18). Pressure surges also do not occur.

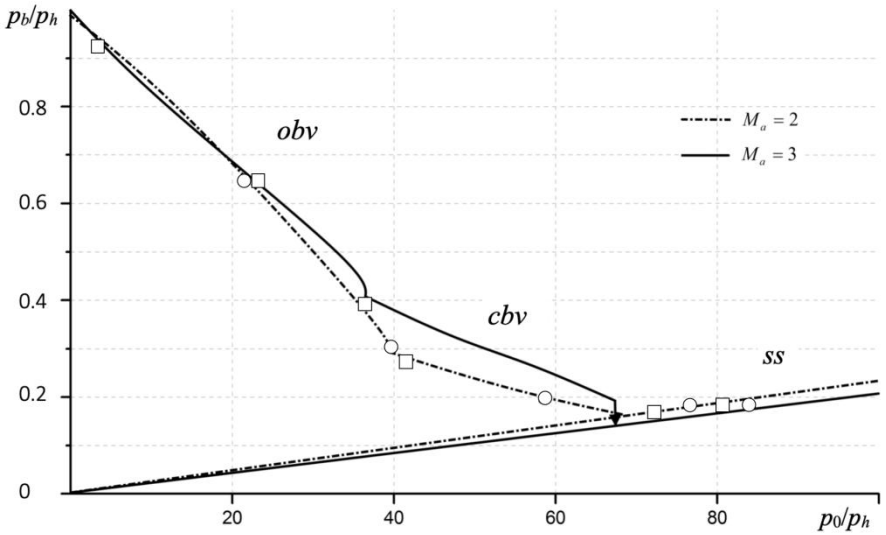

Figure 18. Results of calculations (lines) and experiments (symbols ○ and □) with the outflow of a supersonic jet into a channel with a length l_{tb}=9.71

Non-oscillating restructuring of the shock-wave structure of the jet flowing into the channel from nozzles with a large nozzle half-opening angle occurs at all Mach numbers in the interval M_a=2–4. Thus, for truncated central bodies of aerospike nozzles, a half opening angle θ_a>40° can be recommended. For layouts of the type in Figure 1a, it is recommended to perform the central nozzle also with θ_a>40°, and position the peripheral nozzles in such a way that the length of the equivalent pipe formed by the peripheral jets is more than 10 gauges.

4.6. Annular jet

Figure 19 shows the calculations of the shock-wave structure of a jet flowing out from an annular nozzle with M_a=2 into a channel with a sudden expansion. Nozzle half-opening angle is θ_a=8°. Other geometrical parameters are fixed at l_{tb}=4.02, d_{tb}=85 mm. Total pressure varies from 3 to 10 bar, and total temperature of air equals 300 K. In contrast to the case of a jet outflow from a round Laval nozzle, here we have two base regions: central and peripheral, respectively, for each of them there will be its own plot of $p_b(p_0)$ dependence.

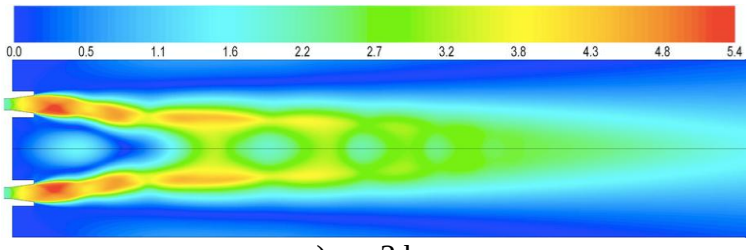

a) p_0=3 bar

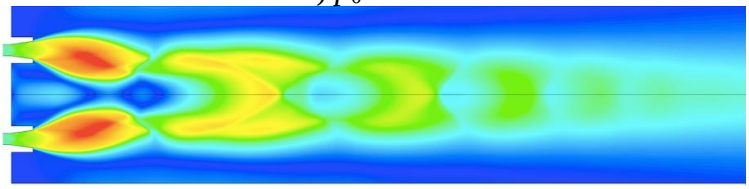

b) p_0=5 bar

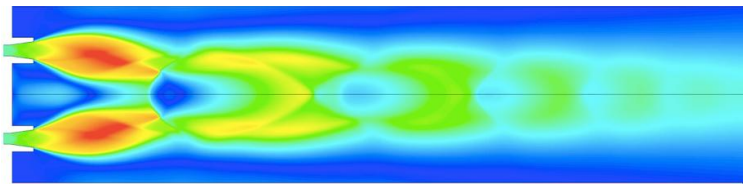

c) p_0=6 bar

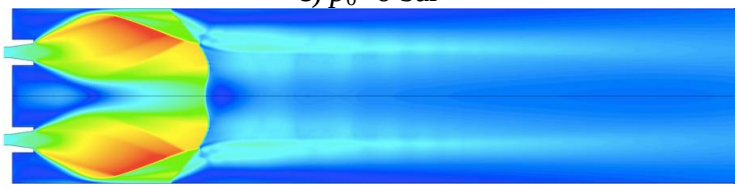

d) p_0=8 bar

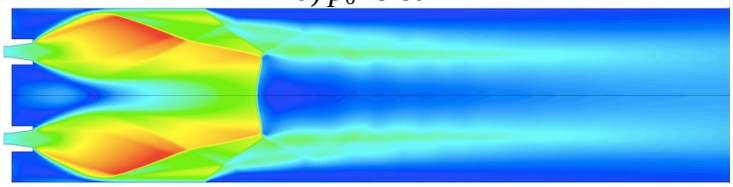

e) p_0=10 bar

Figure 19. Patterns of the outflow of a jet from an annular nozzle with M_a=2 into a channel with a sudden expansion at various values of the total pressure in front of the nozzle

The inner (central) base area becomes closed almost immediately after the nozzle is launched (Figure 19). At p_0=3 bar, the mixing layer on the inner side of the annular jet closes on the axis of symmetry (Figure 19a). At p_0=5 bar, segments of the annular jet with a supersonic flow rate begin to interact with each other (Figure 19b). As a result, a central shock is formed on the jet axis. This corresponds to the minimum pressure in the central base area. At higher values of total pressure (Figures 19c–e), the base pressure increases linearly, because the inner base region turns out to be separated from the environment by regions with a supersonic flow. Therefore, the base pressure does not depend on the outer one. The peripheral base area remains open for a long time, because as total pressure increases, the jet first turns toward the symmetry axis due to a decrease in the size of the central base region. This continues until the value p_0=7 bar, when the central base region switches to a self-similar regime and its dimensions do not change in the future. From this moment, the dimensions of the outer boundary of the annular jet begin to increase; accordingly, the dimensions of the peripheral base region decrease.

It is interesting to compare the $p_b(p_0)$ plots in the peripheral base region of the annular jet and in the usual base region formed when an axisymmetric jet outflows from the Laval nozzle into a cylindrical channel (Figure 20). The transition to the non-self-similar flow mode with a closed base region occurs at higher values of total pressure, the duration of the oscillatory cycle is shorter, and the base pressure in the self-similar mode is larger. The transition from the descending branch of the graph to the ascending one can occur smoothly or be accompanied by an abrupt change in base pressure.

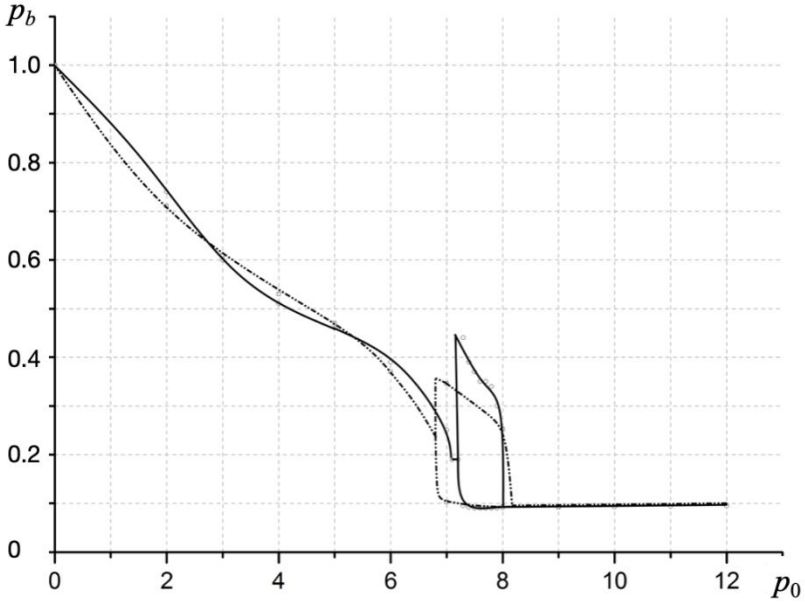

Figure 20. Dependence of base pressure on total pressure for the peripheral base region (solid line) of the annular jet and the usual base region (dashed line) arising during the outflow of an axisymmetric jet into the cylindrical channel

It is also interesting to note that the annular jet has a long, albeit weakly pronounced, transition section between the low-frequency oscillation regime and the self-similar regime, when $p_b(p_0)$ dependence remains non-linear, while for an axisymmetric jet it becomes linear immediately after the point of minimum base pressure. This phenomenon is explained by the separation of the outer boundary of the annular jet from the channel walls (Figures 19d, e). Perturbations from the environment through the boundary layer in the separation region penetrate into the peripheral base region. In the regime with a closed base region, the flow patterns of the annular and ordinary jets are similar.

5. Conclusion

The study of flows in a channel with sudden expansion is of interest for the development of complex technical devices in which separated flows are observed (nozzle blocks, ejectors, combustion chambers with supersonic combustion). The interaction of supersonic jets emanating from a multi-nozzle block leads to complex three-dimensional separated flows. In a separated flow with a sudden expansion, a base region is distinguished, in which, due to the ejecting action of the jet (or external supersonic flow), the characteristic pressure is lower than in the environment or in the main (cocurrent) flow. The outflow into the channel with a sudden expansion is accompanied by a change in the flow regimes, both stationary and unsteady.

The dependences of the peripheral base pressure and base pressure in the central part are investigated. The value of the base pressure in the central part remains constant, while the value of the base pressure in the peripheral region is variable in unsteady flow regimes. The dependence of the peripheral base pressure for an annular nozzle has a shape similar to the dependence of the base pressure for a single axisymmetric jet with the same nozzle throat area. It is possible to achieve a smooth non-oscillating launch in aerospike nozzles. For this, in multi-nozzle arrangements, the half-opening angle should be θ_a>40° at the central nozzle or at the truncated central body in aerospike nozzles. This recommendation is valid for nozzles with Mach numbers from 2 to 4.

Numerical methods based on differential models of turbulence make it possible to simulate the oscillations of shock-wave structures in separated flows if the oscillation frequency is significantly less than the frequency of the descent of large turbulent eddies. Comparison of the

results computed with various turbulence models with experimental data show that SST model is the most suitable turbulence model to study unsteady flows arising in the nozzle devices of rocket engines. The calculations performed correctly reproduce the basic regularities of the dependence of the base pressure on the total pressure, three types of oscillations, and transition from one type of oscillation to another.

The results obtained can be useful in the study of supersonic gas jets, interference of gas-dynamic discontinuities, pressure fluctuations in elements of aerospace technology, oscillations of shock-wave structures in technological installations, jet and rocket engines.

Acknowledgements

This work was financially supported by the Ministry of Science and Higher Education of Russian Federation during the implementation of the project "Creating a leading scientific and technical reserve in the development of advanced technologies for small gas turbine, rocket and combined engines of ultra-light launch vehicles, small spacecraft and unmanned aerial vehicles that provide priority positions for Russian companies in emerging global markets of the future", No. FZWF-2020-0015.

References

1. Smirnov N.N. Digital space physical space science and technology. Acta Astronautica. 2021. Vol. 181. P. 530-536.
2. Flandro G.A. Effects of vorticity on rocket combustion stability. Journal of Propulsion and Power. 195. Vol. 11. No. 4. P. 607–625.
3. Emelyanov V.N., Teterina I.V., Volkov K.N., Garkushev A.U. Pressure oscillations and instability of working processes in the combustion chambers of solid rocket motors. Acta Astronautica. 2017. Vol. 135. P. 161–171.
4. Korst H.H. A theory for base pressure in transonic and supersonic flow. Journal of Applied Mechanics. 1956. Vol. 23. No. 4. P. 593–600.
5. Hwang C.-B., Chow W.L., Moslemian D. Base pressure of a sudden expansion from a conical converging nozzle. AIAA Journal. 1993. Vol. 31. No. 4. P. 657-662.
6. Jungowski W.M. On the pressure oscillating in a sudden enlargement of a duct section. Fluid Dynamics Transactions. 1967. No. 1. P. 735–741.
7. Jungowski W.M. On the flow in a sudden enlargement of a duct. Fluid Dynamics Transactions. 1969. Vol. 4. P. 231–241.
8. Jungowski W.M., Witczak K.J. Properties of an annular jet generating discrete frequency noise. Archives of Mechanics. 1976. Vol 28. No. 6. P. 847–854.
9. Anderson J.S., Jungowski W.M., Hiller W.J., Meier G.E.A. Flow oscillation in a duct with a restangular cross-section. Journal of Fluid Mechanics. 1977. Vol. 79. P. 769–784.
10. Jungowski W.M. Some self-induced supersonic flow oscillations. Progress in Aerospace Science. 1978. Vol 18. P. 151–175.
11. Meier G.E.A., Grabirz G., Jungowski W.M., Witczak K.J., Anderson J.S., Oscillations of the supersonic flow downstream of a abrupt increase in a duct cross-section. AIAA Journal. 1980. Vol 18. No. 4. P. 394–395.
12. Bulat P. V., Zasuhin O.N., Uskov V.N. On classification of flow regimes in a channel with sudden expansion. Thermophysics and Aeromechanics. 2012. Vol. 19. No. 2. P. 233–246.
13. Xiansheng W., Dangguo Y., Jun L., Fangqi Z. Control of pressure oscillations induced by supersonic cavity flow. AIAA Journal. 2020. Vol. 58. P. 2070–2077.
14. Saleel A., Bai M.A.A., Khan S.A. Experimental investigation of the base flow and base pressure of sudden expansion nozzle. IOP Conference Series: Materials Science and Engineering. 2018. Vol. 370. 012052.

15. Pathan K.A., Dabeer P.S., Khan S.A. Optimization of area ratio and thrust in suddenly expanded flow at supersonic Mach numbers. Case Studies in Thermal Engineering. 2018. Vol. 12. P. 696–700.
16. Afzal A., Khan S.A., Islam M.T., Jilte R.D., Khan A., Soudagar M.E.M. Investigation and back-propagation modeling of base pressure at sonic and supersonic Mach numbers. Physics of Fluids. 2020. Vol 32. No. 9. 096109.
17. Raje P.V., Sinha K. Three-dimensional simulation of rocket nozzles with multi-jet interaction using shock-unsteadiness model. AIAA Paper. 2019. No. 2019-3322.
18. Morinigo J.A., Salva J.J. Three-dimensional simulation of the self-oscillating flow and side-loads in an over-expanded subscale rocket nozzle. Proceedings of the Institution of Mechanical Engineers. Part G. Journal of Aerospace Engineering. 2006. Vol. 220. No. 5. P. 507–523.
19. Lefrancois E., Frequency dependency of side loads resulting from shock motion in a forced oscillating rocket nozzle. Computers and Fluids. 2011. Vol. 49. No. 1. P. 222–232.
20. He M., Qin L., Liu Y. Numerical investigation of flow separation behavior in an over-expanded annular conical aerospike nozzle. Chinese Journal of Aeronautics. 2015. Vol. 28. No. 4. P. 983–1002,
21. Kirchheck D., Saile D., Gülhan A. Spectral analysis of rocket wake flow-jet interaction by means of high-speed schlieren imaging. Proceedings of the 8th European Conference for Aeronautics and Aerospace Sciences (EUCASS2019), 1-4 July 2019, Madrid, Spain. 2019. No. 1057.
22. Ivanov I.E., Kryukov I.A. Numerical study of ways to prevent side loads in an overexpanded rocket nozzles during the launch stage. Acta Astronautica. 2019. Vol. 163. Part A. P. 196–201.
23. Ferrero A., Martelli E., Nasuti F., Pastrone D. Fluidic control of transition in a dual-bell nozzle. AIAA Paper. 2020. No. 2020-3788.
24. Ferrero A., Conte A., Martelli E., Nasuti F., Pastrone D. Dual-bell nozzle for space launchers with fluidic control of transition. AIAA Paper. 2021. No. 2021-3586.
25. Seidl M.J., Aigner M., Keller R., Gerlinger P. CFD simulations of turbulent non-reacting and reacting flows for rocket engine applications. The Journal of Supercritical Fluids. 2017. Vol. 121. P. 63–77.
26. Bai X., Cheng P., Li Q., Sheng L., Kang Z. Effects of self-pulsation on combustion instability in a liquid rocket engine. Experimental Thermal and Fluid Science. 2020. Vol. 114. 110038.
27. Smirnov N.N., Betelin V.B., Shagaliev R.M., Nikitin V.F., Belyakov I.M., Deryuguin Yu.N., Aksenov S.V., Korchazhkin D.A. Hydrogen fuel rocket engines simulation using LOGOS code. International Journal of Hydrogen Energy. 2014. Vol. 39. No. 20. P. 10748–10756.
28. Volkov K.N., Emelyanov V.N., Efremov A.V., Tsvetkov A.I. Flow structure and pressure oscillations during the interaction of a supersonic underexpanded gas jet with a tubular cavity. Technical Physics. 2020. Vol. 65. No. 8. P. 1204-1216.
29. Volkov K.N., Emelyanov V.N., Efremov A.V., Tsvetkov A.I. Acoustic characteristics of the self-excited oscillating process, arising from the interaction of supersonic under-expanded jet with a cylindrical cavity. Technical Physics. 2020. Vol. 65. No. 5. P. 703-709.
30. Emelyanov V., Karpenko A., Volkov K. Development and acceleration of unstructured mesh based CFD solver. Progress in Flight Physics. 2017. Vol. 9. P. 387–408.
31. Silnikov M.V., Chernyshov M.V., Uskov V.N. Two-dimensional over-expanded jet flow parameters in supersonic nozzle lip vicinity. Acta Astronautica. 2014. Vol. 97. P. 38–41.
32. Silnikov M.V., Chernyshov M.V., Uskov V.N. Analytical solutions for Prandtl–Meyer wave – oblique shock overtaking interaction. Acta Astronautica. 2014. Vol. 99. P. 175–183.
33. Silnikov M.V., Chernyshov M.V. The interaction of Prandtl–Meyer wave and quasi one dimensional flow region. Acta Astronautica. 2015. Vol. 109. P. 248–253.

34. Bulat P., Volkov K., Volobuev I. Interaction between shock waves travelling in the same direction. Fluids. 2021. Vol. 6. No. 9. 315 (18 pages).
35. Bulat P., Melnikova A., Upyrev V., Volkov K. Refraction of oblique shock wave on a tangential discontinuity. Fluids. 2021. Vol. 6. No. 9. 301 (24 pages).